XXVIII. Erfahrungsaustausch
Oberflächentechnologie mit Plasma- und Ionenstrahlprozessen
Mühlleithen, 13. - 16. März 2023

Progress of the Electric Propulsion Diagnostic Package (EPDP)

V. Schneider[1], T. Trottenberg[1], H. Kersten[1], J. Laube[2], H. Henkel[3] and R. Wimmer-Schweingruber[1]

[1]Institute of Experimental and Applied Physics, Christian-Albrechts-University Kiel
[2]OHB System AG, Bremen
[3]von Hoerner & Sulger GmbH, Schwetzingen

Motivation: Why do we need diagnostics for electrically propelled spacecrafts?

Motivation

Deep Space 1
NASA

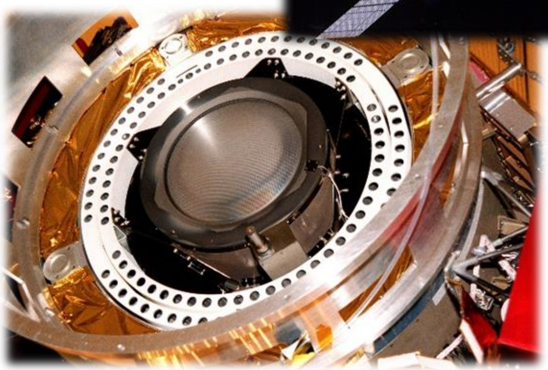

SMART-1
ESA

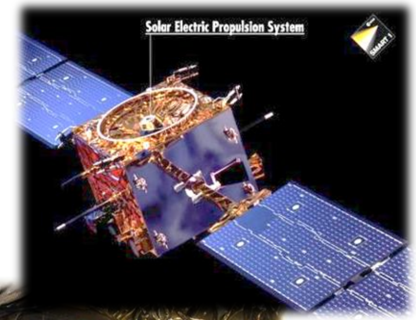

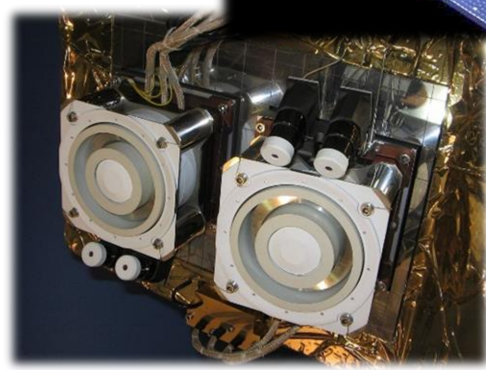

- Gridded Ion Thruster
- 0.1 µA/cm² ion flux near thruster exit
- Deposition of molybdenum: ~ 1 nm / 100 h (line-of-sight)

- Hall Thruster
- Ion energies: e.g. 35 eV (peak) tale up to 90 eV
- Energies vary along the orbit
- Floating potential of cathode:
- -5 V to +10V

Wang et al., "*Deep Space One Investigations of Ion Propulsion Plasma Environment*", J. Spacecr. Rockets **37**, 545 (2000)

Brinza et al., "*Deep Space 1 Measurements of Ion Propulsion Contamination*", J. Spacecr. Rockets **38**, 426 (2001)

González del Amo, et al., "*Spacecraft/thrusters interaction analysis for Smart-1*", IEPC–2005–003 (2005)

Motivation

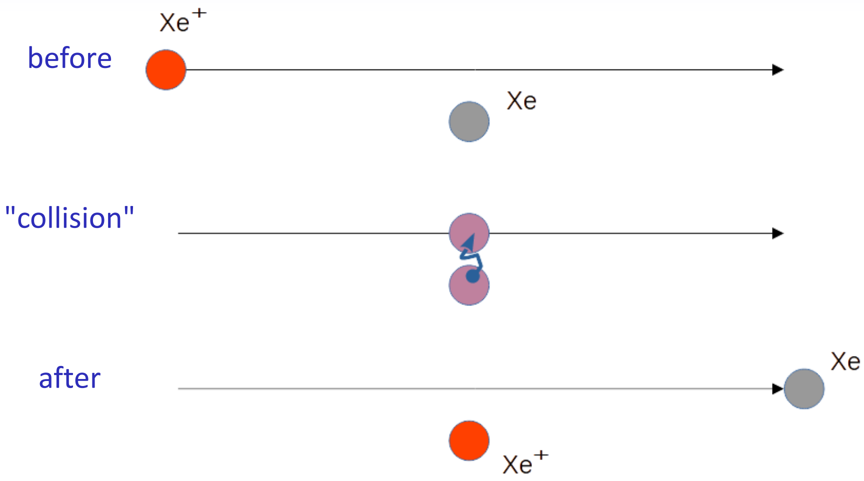

- charge-exchange collisions produce a secondary plasma around the spacecraft

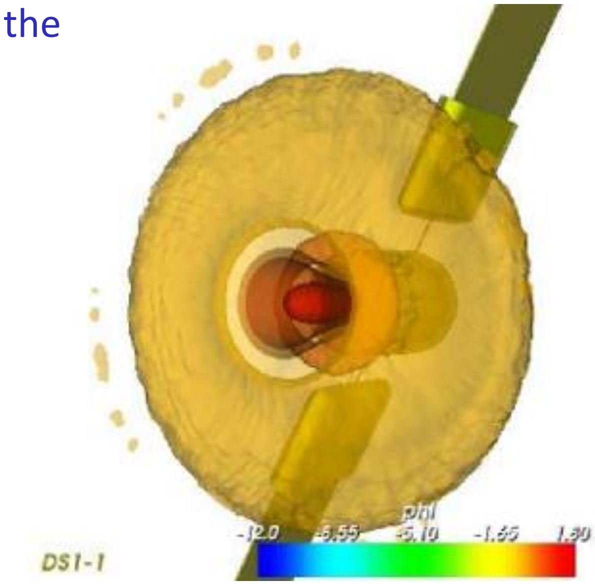

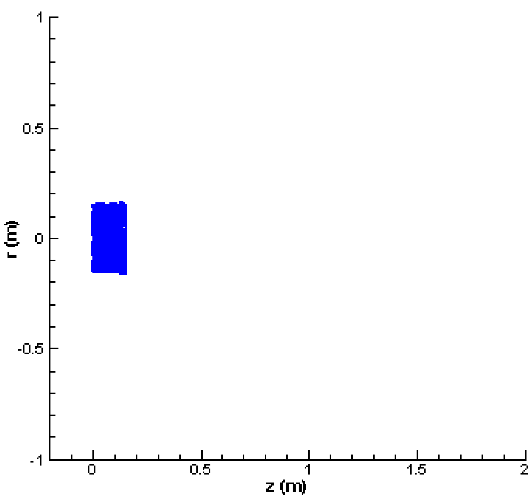

- unpredictable effects due to local electric fields
- disturbance of measurements and (radio-) communication
- possible destructive arcing
- backflow from thruster to spacecraft very hard to assess from ground experiments

Roy, R.S., "*Numerical Simulation of Ion Thruster Plume Backflow for Spacecraft Contamination Assessment*", PhD Dissertation, MIT (1995)

Wang, J. et al., "*Three-Dimensional Particle Simulation Modeling of Ion Propulsion Plasma Environment for Deep Space One*", J. Spacecr. Rockets **38**, 433 (2001)

Brieda, L. et al., "*Development of A Virtual Testing Environment for Electric Propulsion*", AIAA-2003-5020 (2003)

The EPDP for the Heinrich Hertz Satellite

The Spacecraft H^2SAT

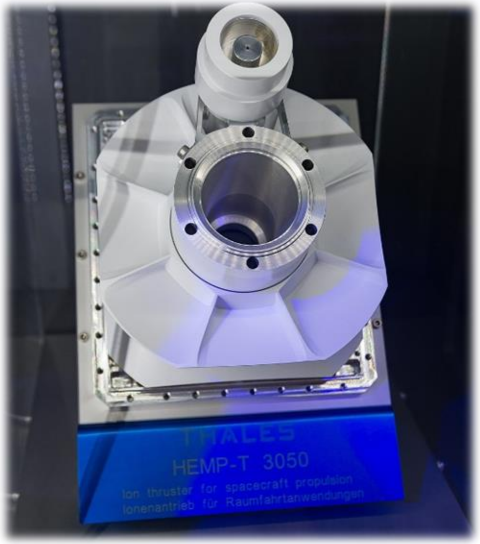

HEMP-T 3050
Thales Deutschland GmbH

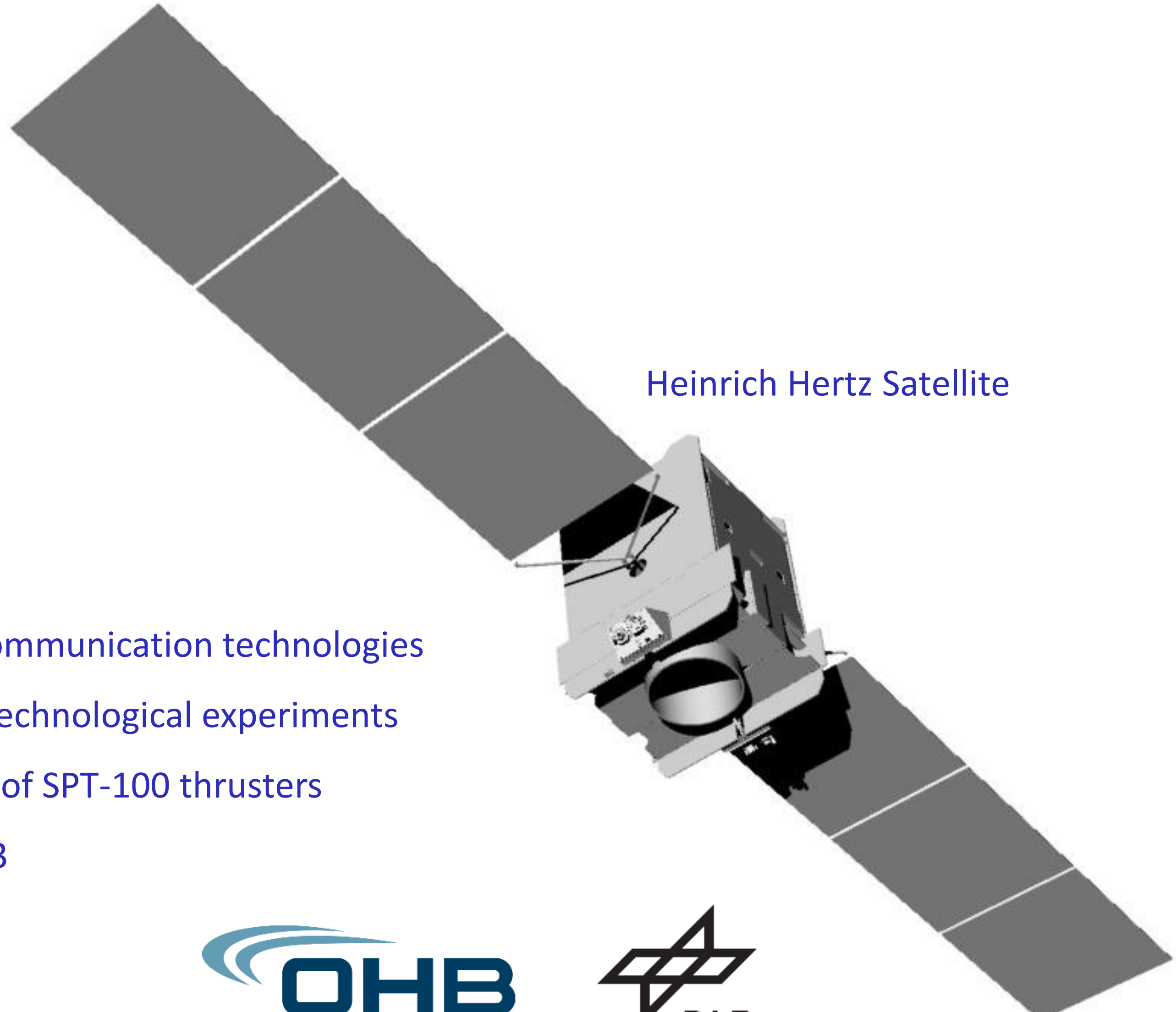

Heinrich Hertz Satellite

- explore and test new telecommunication technologies
- platform for scientific and technological experiments
- pair of HEMP-T 3050 + pair of SPT-100 thrusters
- to be launched in June 2023
- financed by DLR
- integrated by OHB

The EPDP Sensors

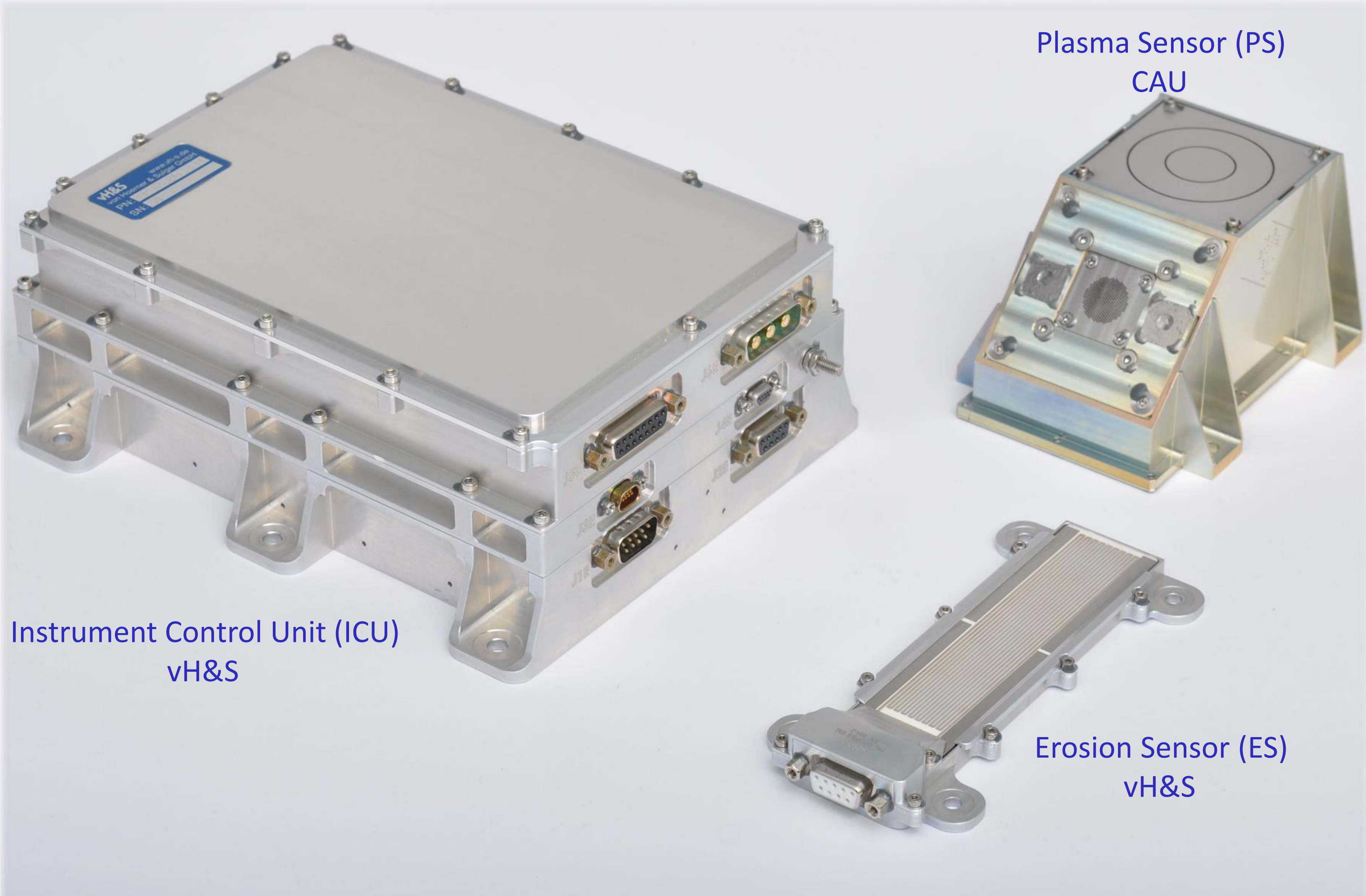

Sensors on the Satellite

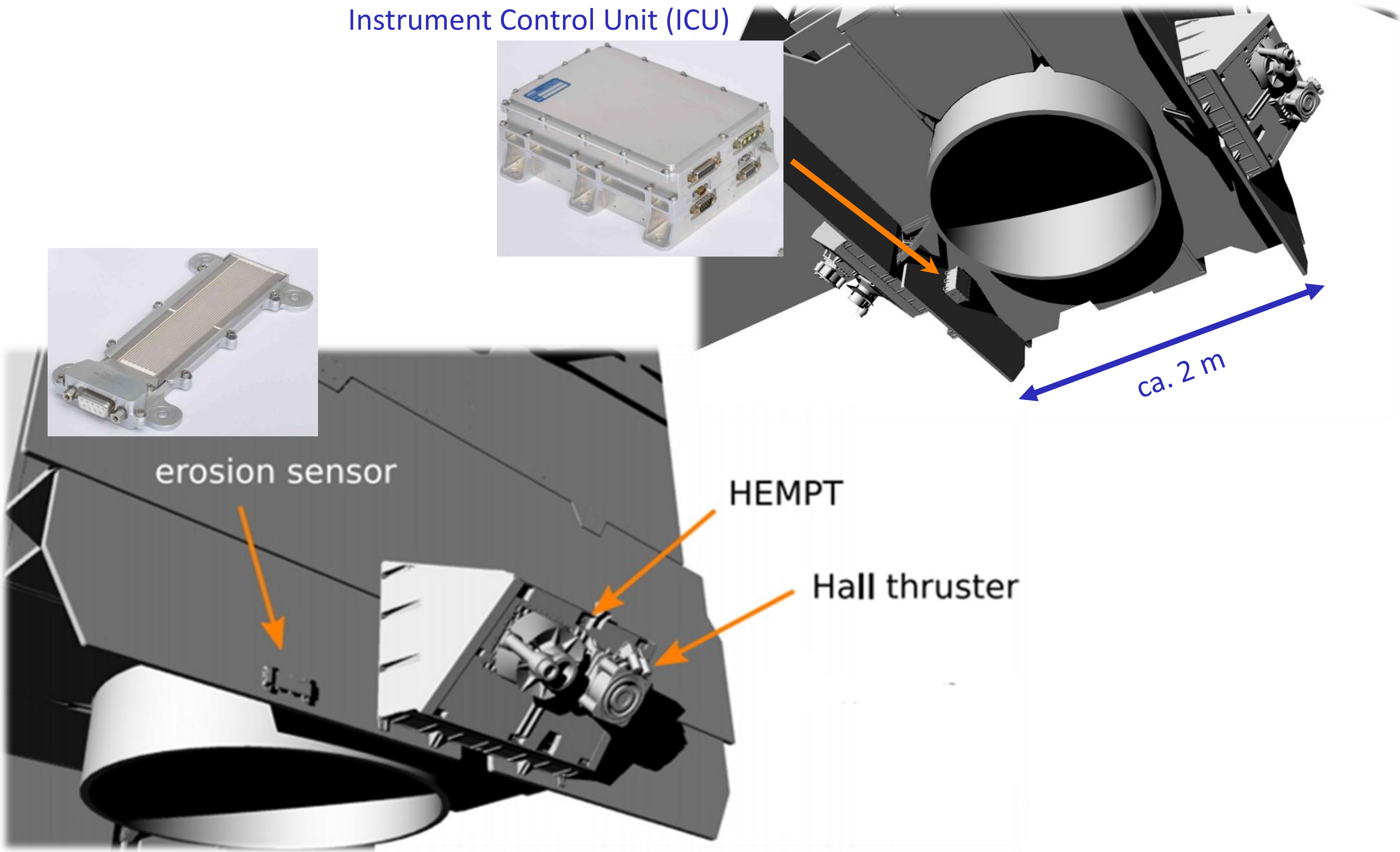

Sensors on the Satellite

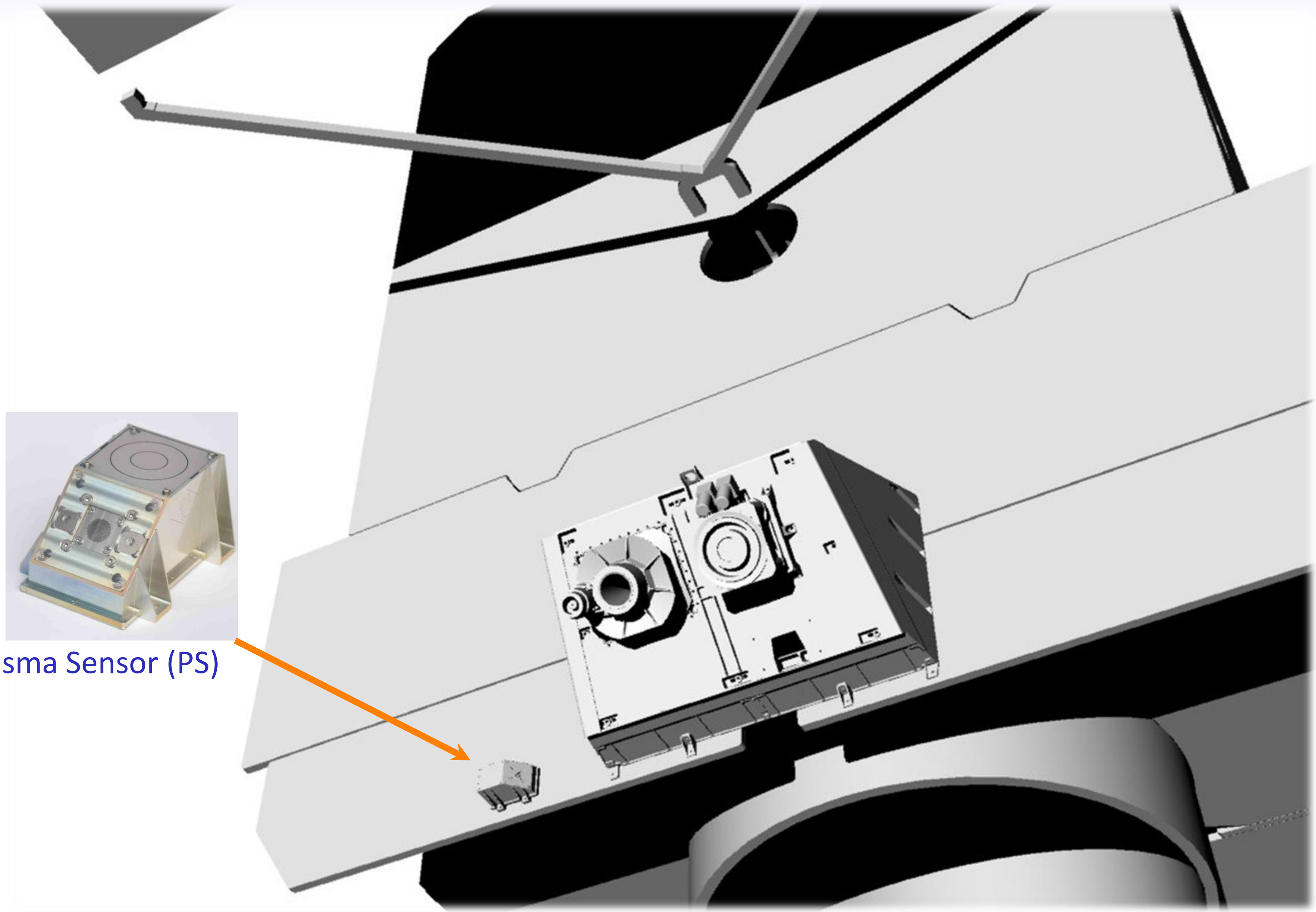

Plasma Sensor

Retarding Potential Analyzer

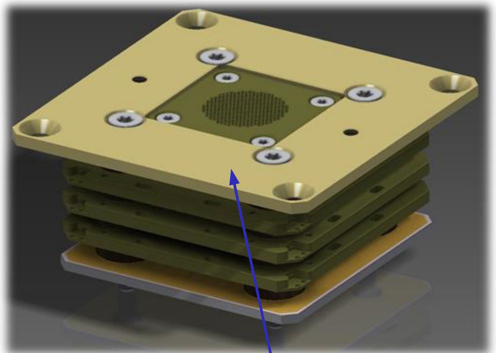

@S/C-potential

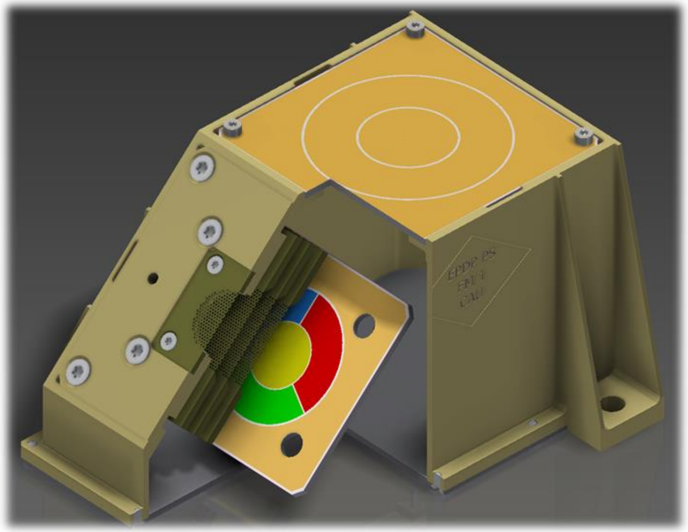

Langmuir Probe

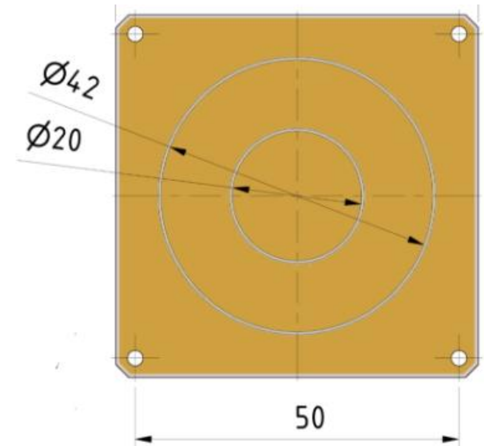

- probe area: $A = 3.1cm^2$
- saturation currents:

$$I_e = 0.4\ \mu A \dots 90\ \mu A$$

$$I_i = 2\ nA \dots 0.5\ \mu A$$

- simulations:

$$n_e = (5 \cdot 10^{10} \dots 1 \cdot 10^{13})\ m^{-3}$$

$$k_B T_e = 3\ eV$$

→ screening length

$$\lambda_{De} = \left(\frac{k_B T_e}{n_e {e_0}^2} \right) = 4\ mm \dots 6\ cm$$

entrance grid

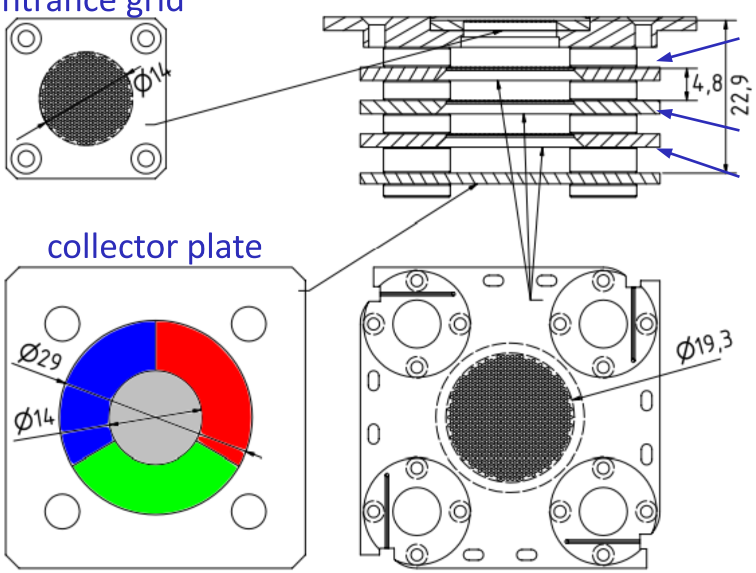

repelling grid, typ. -20 V

discriminating grid

repelling grid, typ. -20 V

- four titanium grids
- segmented collector
- 0.5 mm holes
- 0.2 mm separated

Erosion Sensor

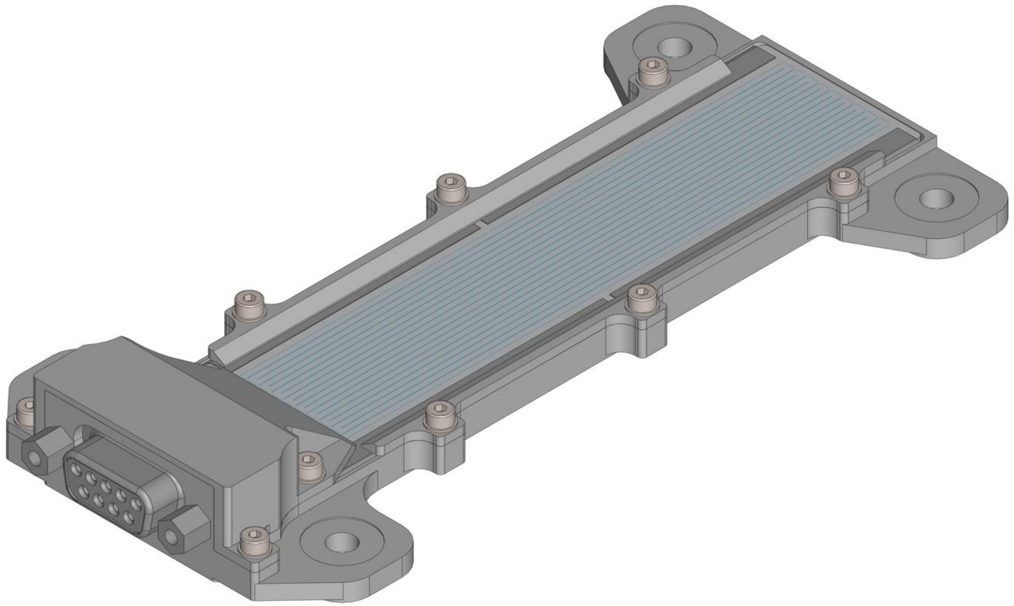

- resistance measurement
- Ag-meander:
  - 180 cm long
  - 2 µm thick
  - 1 mm wide
  - ~30 Ω

- hardware is simpler than QCM but data evaluation is more challenging:
  - temperature drifts -80 ... +110 °C
  - additional currents from plasma (thruster-generated, solar wind)
  - electromagnetic interference from the HEMP-T ?
    - ⇒ filtering and AC measurement techniques

Plasma Performance Tests For The Flight Model

Test Environment

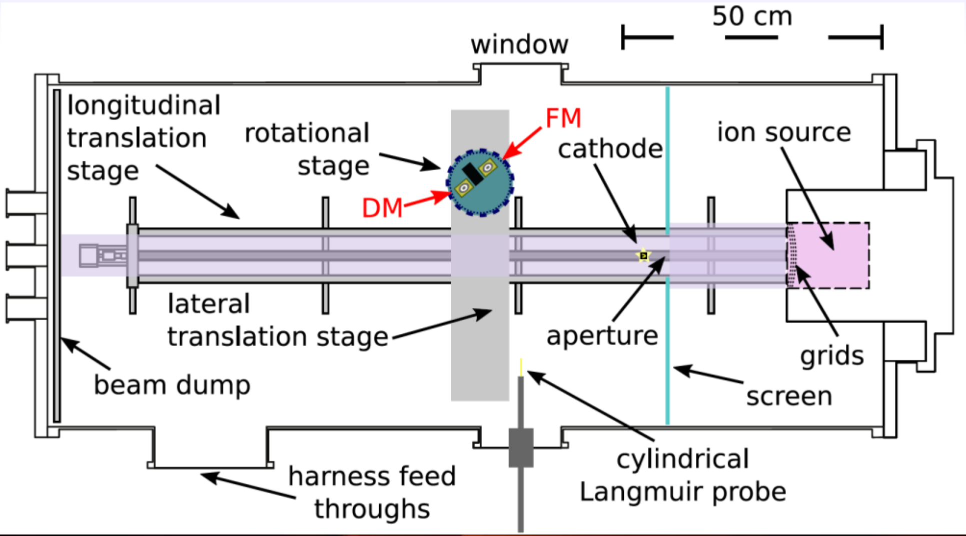

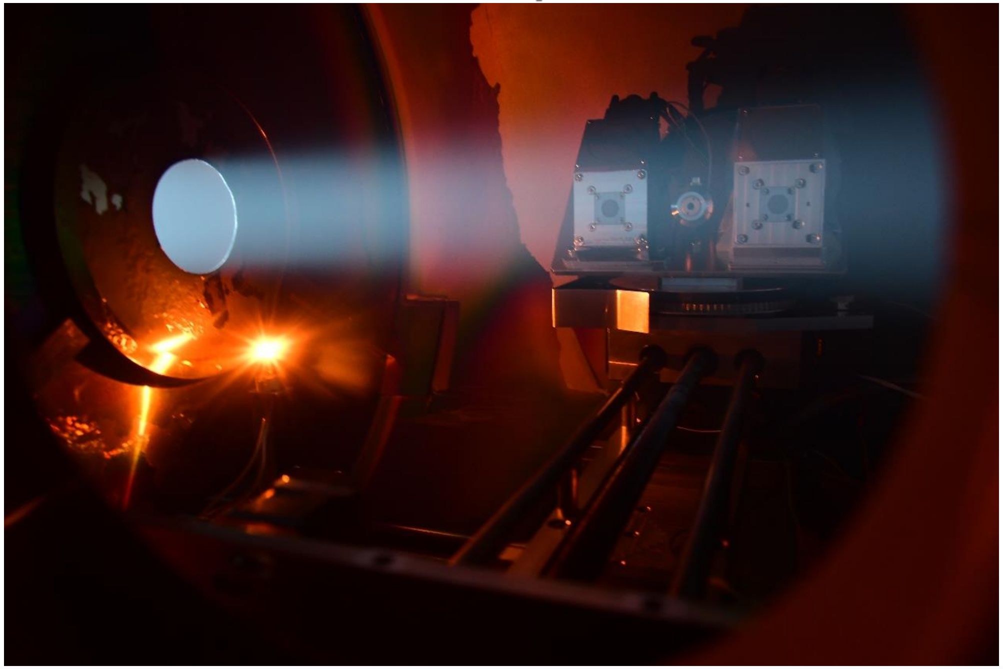

- mimic the plasma environment at a satellite with electric propulsion
- the sensors measure the dilute backflow from the thruster plume that alters or dominates the plasma surrounding the spacecraft
- directional characteristic of the RPA
- calibrate the current densities measured by the RPA
- assure that the Flight Model (FM) and the Demonstrator Model (DM) generate reasonably comparable data
- assure that the FM has not been degraded by the environmental tests (thermal and shaking)

Measurements parallel to a 1.2 keV ion beam

LP

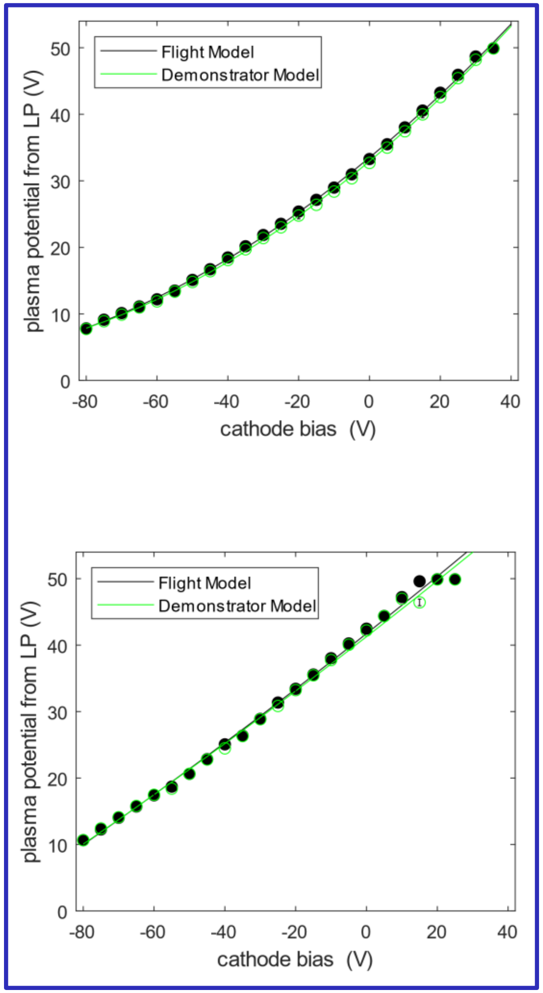

RPA

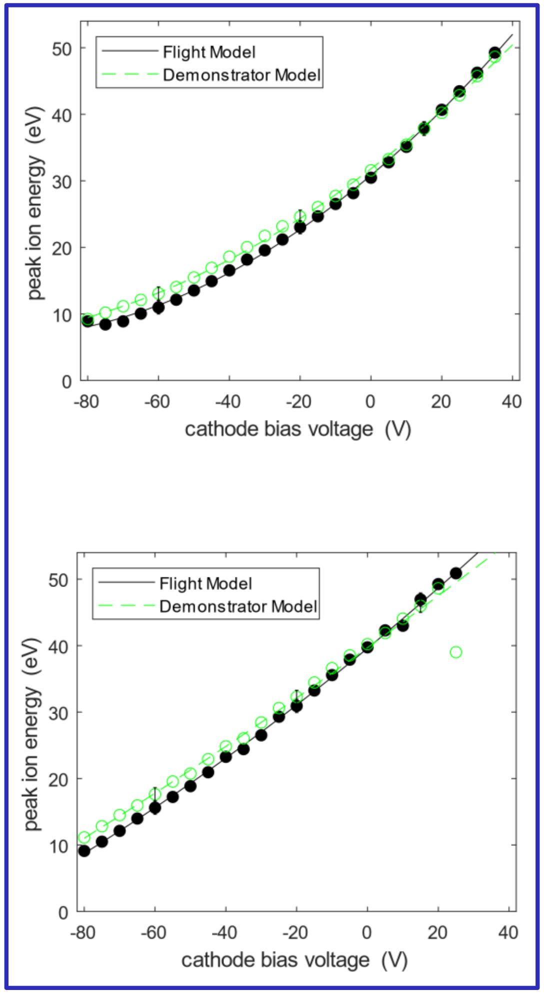

before shake & bake

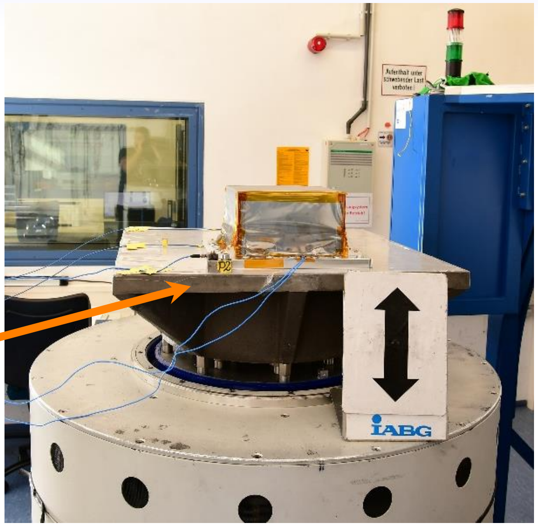

after shake & bake

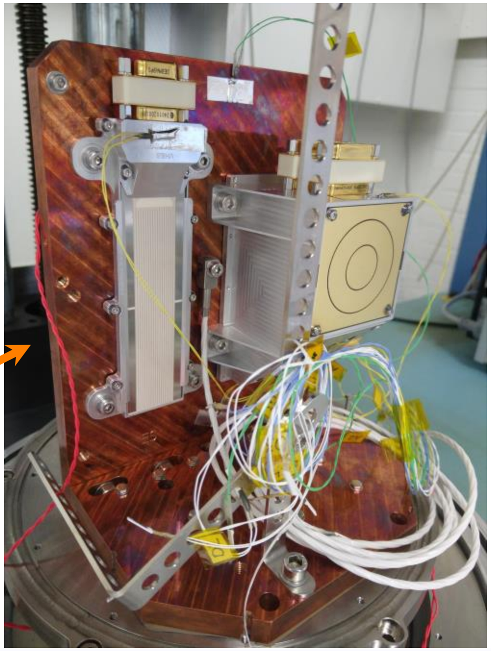

Measurements parallel to a 1.2 keV ion beam

RPA characteristics

FM

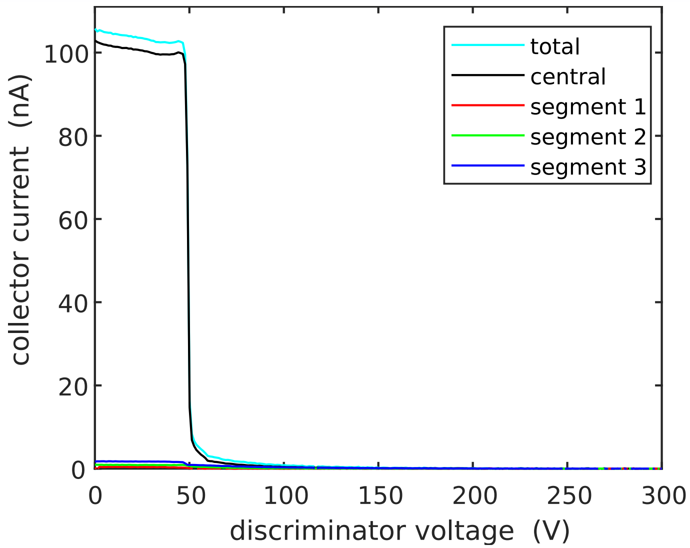

DM

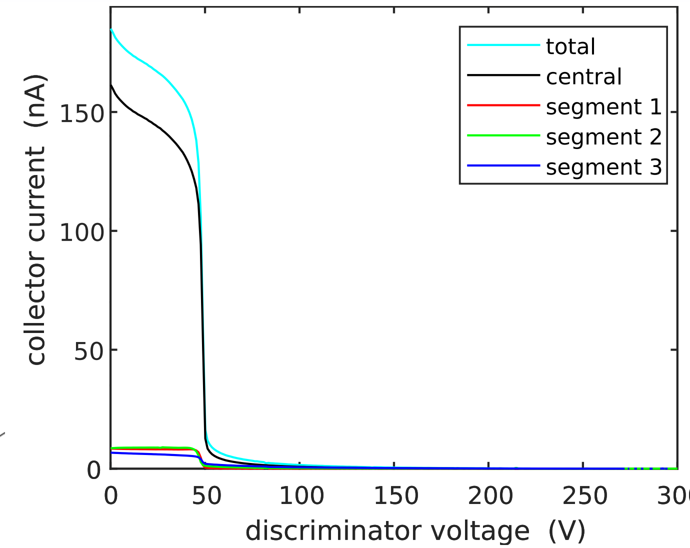

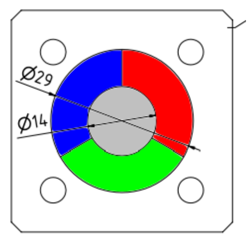

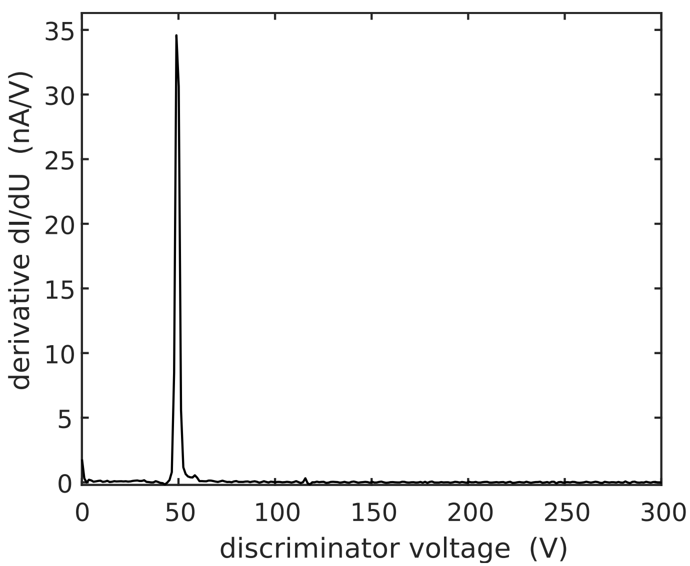

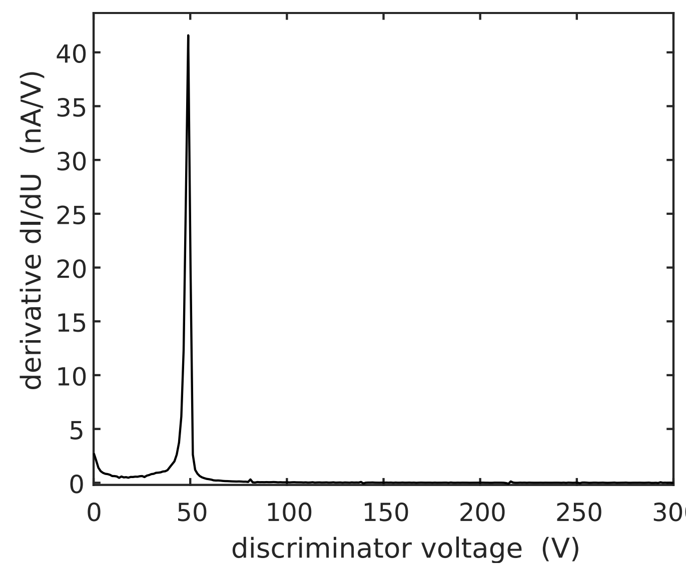

Measurements in the idling beam

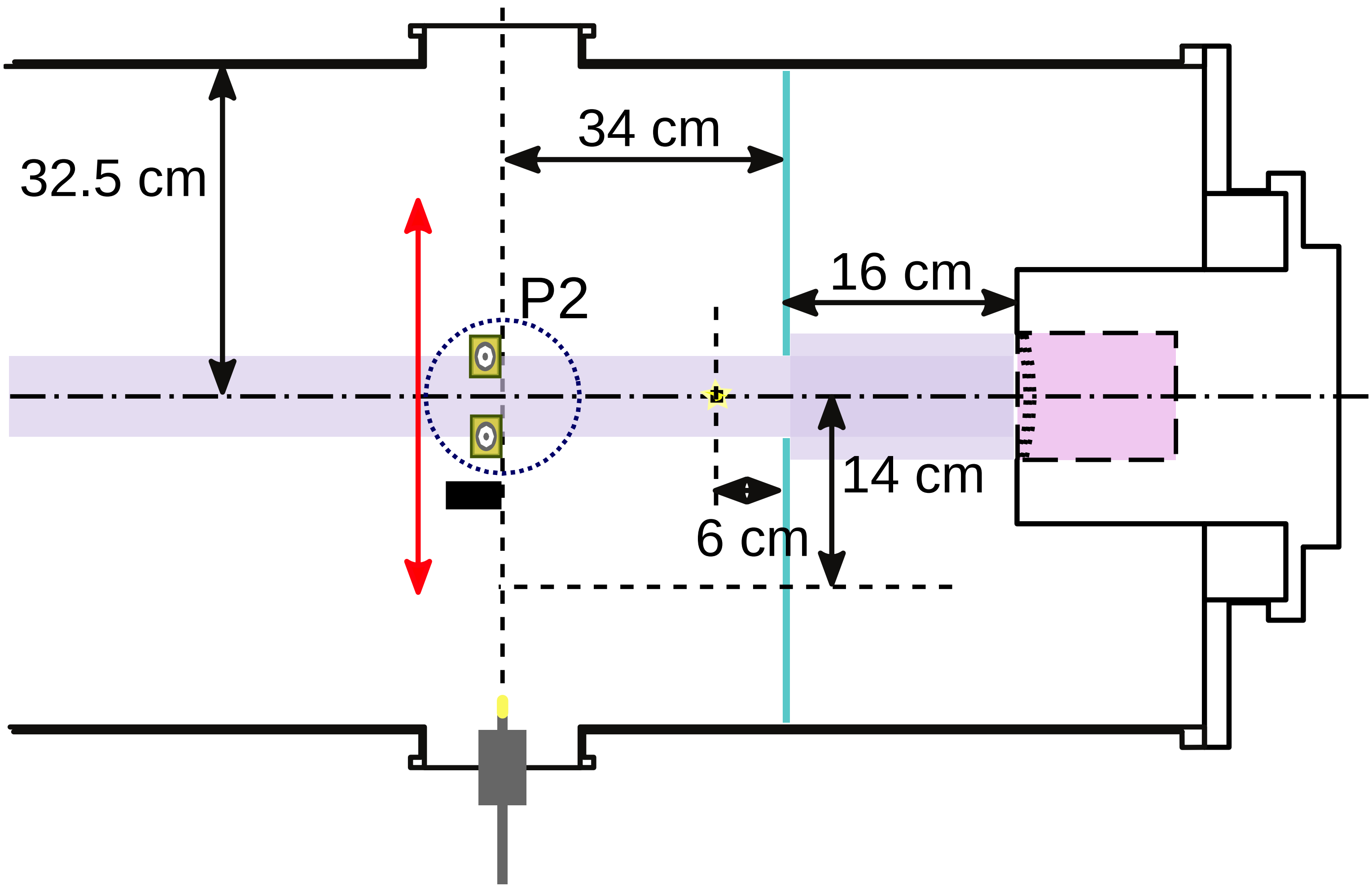

Measurements in the idling beam

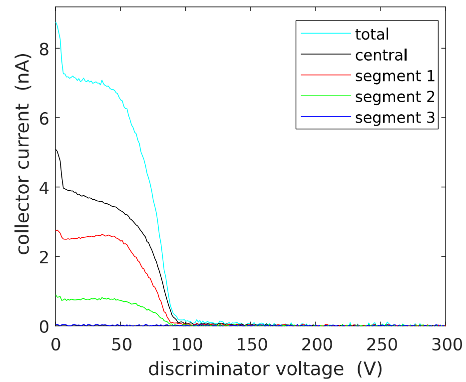

(a) FM, $r = -14\,\mathrm{cm}$, (outside beam, left).

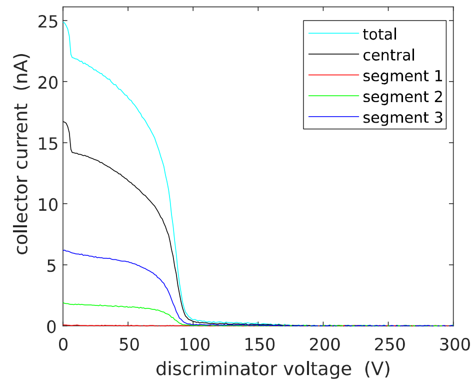

(b) FM, $r = +10\,\mathrm{cm}$, (beam edge, right).

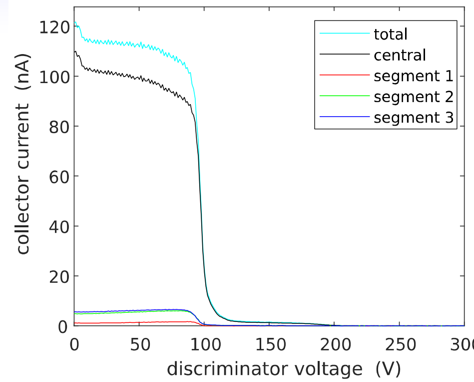

(c) FM, $r = 0\,\mathrm{cm}$, (beam center).

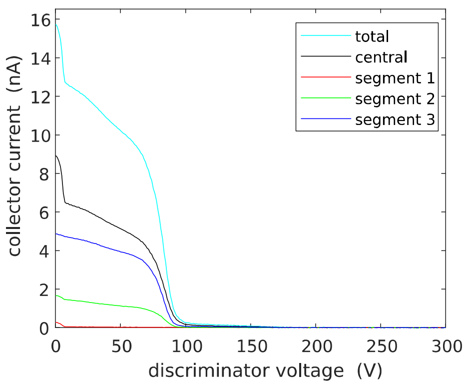

(d) DM, $r = +14\,\mathrm{cm}$, (outside beam, right).

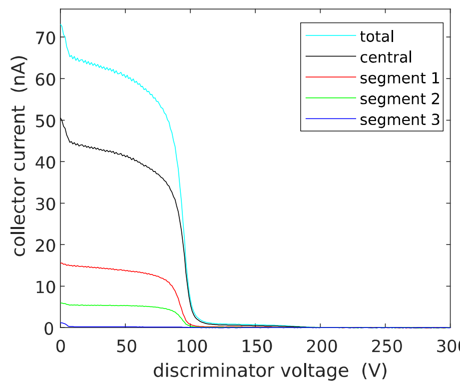

(e) DM, $r = -10\,\mathrm{cm}$, (beam edge, left).

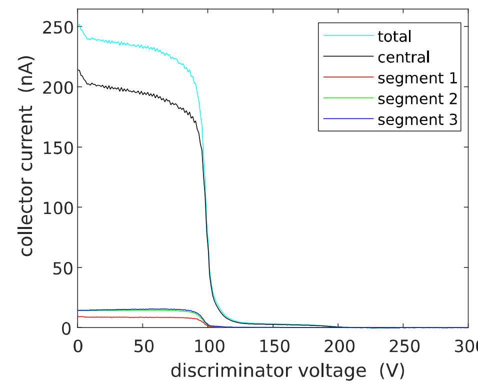

(f) DM, $r = 0\,\mathrm{cm}$, (beam center).

- Measurements across the idling beam after the environmental tests. RPA characteristics of both sensors.
- Cathode bias: U_{cath} = 0 V, sensor position: z = 34 cm, sensor direction: α = 0°.

Measurements in the idling beam

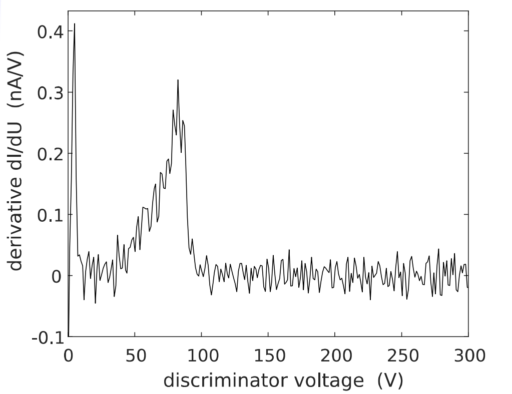

(a) FM, $r = -14\,\mathrm{cm}$, (outside beam, left).

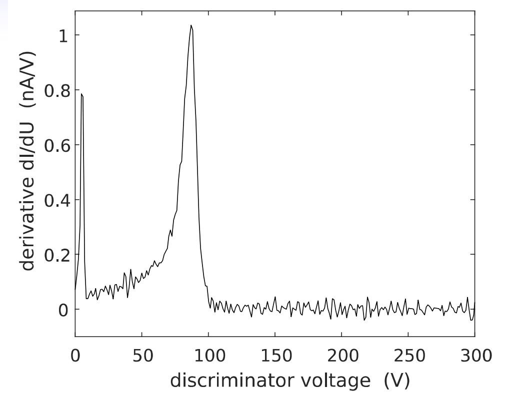

(b) FM, $r = +10\,\mathrm{cm}$, (beam edge, right).

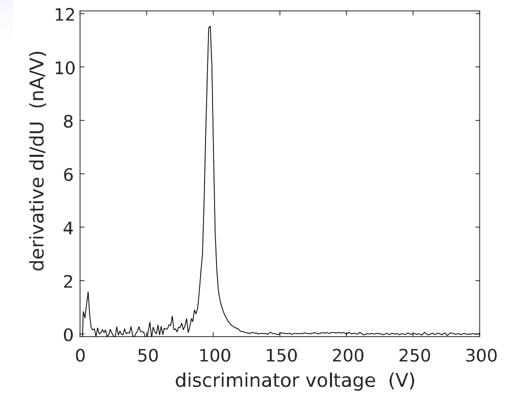

(c) FM, $r = 0\,\mathrm{cm}$, (beam center).

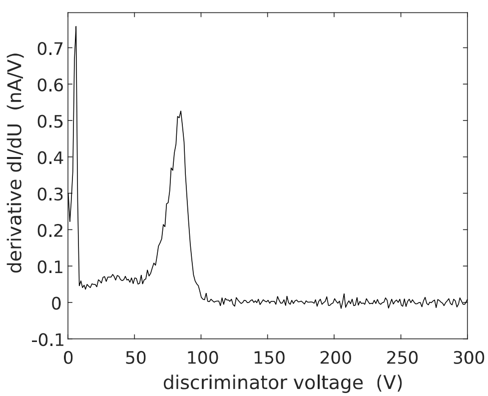

(d) DM, $r = +14\,\mathrm{cm}$, (outside beam, right).

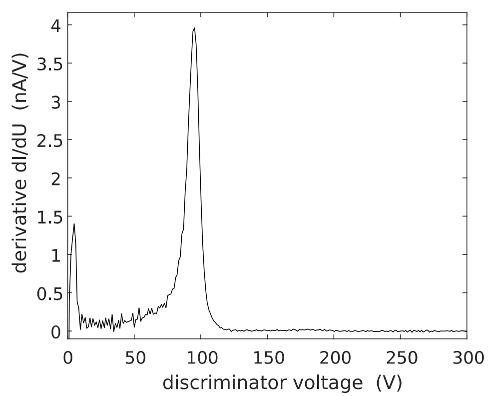

(e) DM, $r = -10\,\mathrm{cm}$, (beam edge, left).

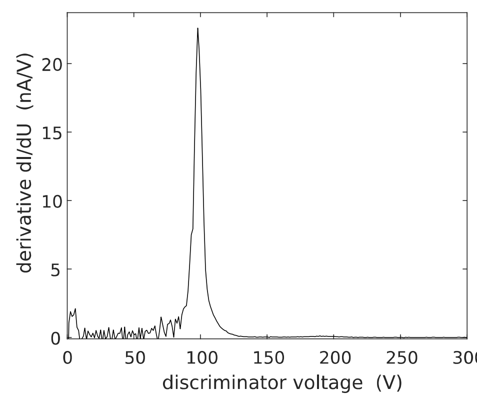

(f) DM, $r = 0\,\mathrm{cm}$, (beam center).

- RPA derivatives of both sensors

Comparison with Faraday cup measurements

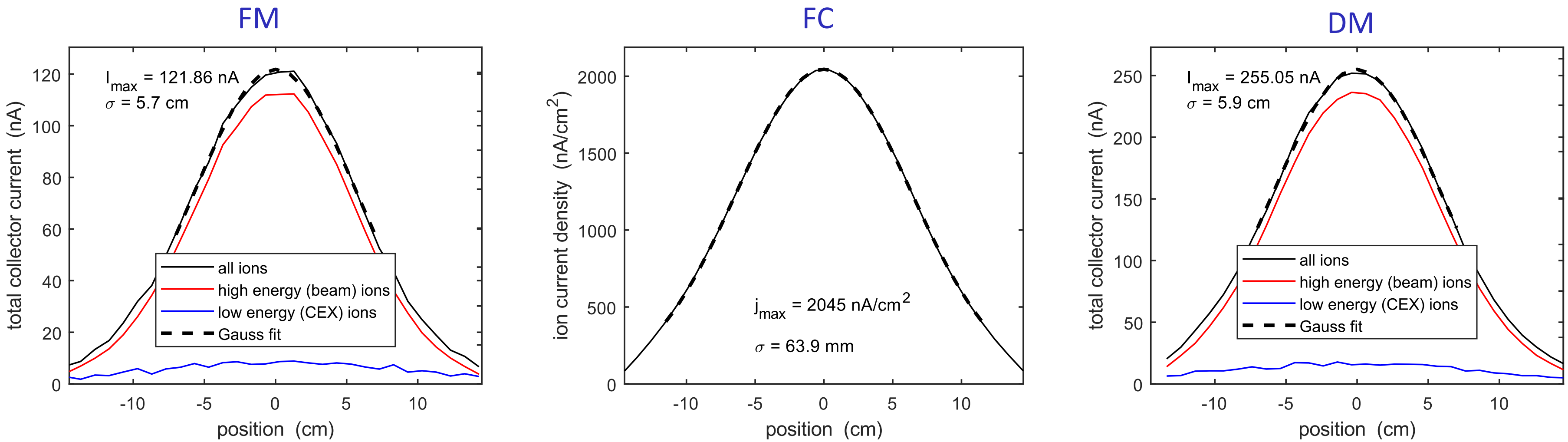

- Faraday cup measurements at the same positions where the RPA measured in order to provide a “calibration” of the EPDP RPA
- total current at a discriminator grid voltage of 0 V as the black curve
- red curve depicts the total current at a discriminator grid voltage of 40 V --> only ions with kinetic energies that exceed 40 eV can pass through the discriminator grid
- difference between both, i.e. the ions with kinetic energies less than 40 eV, is plotted as the blue curve

RPA directivity measurements

- idling ion beam
- central position
- rotation ±36°

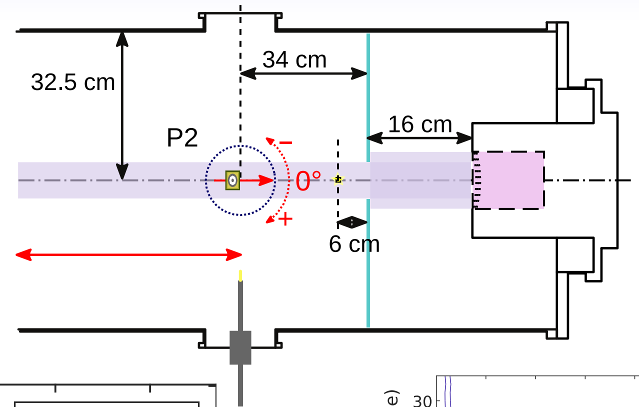

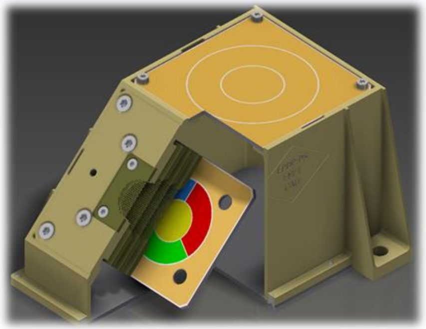

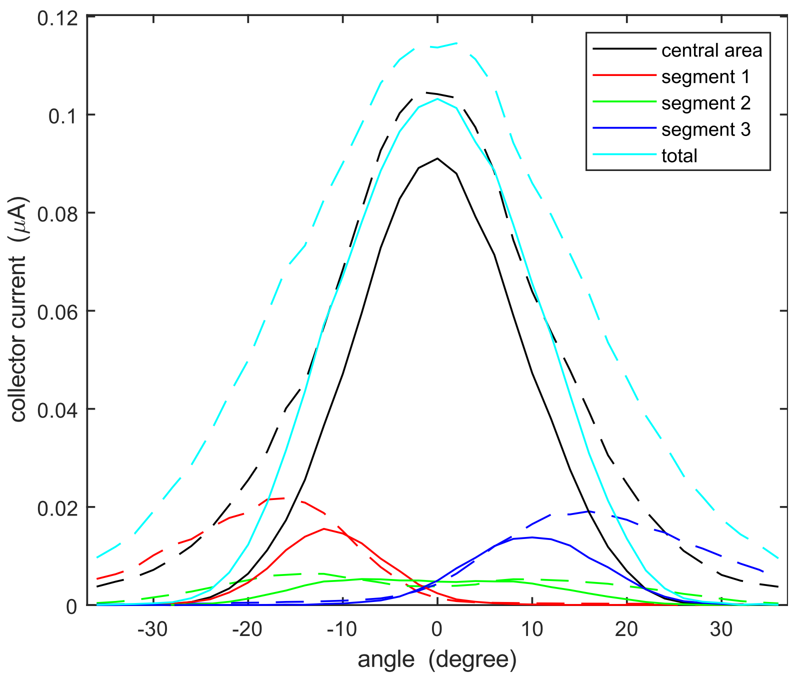

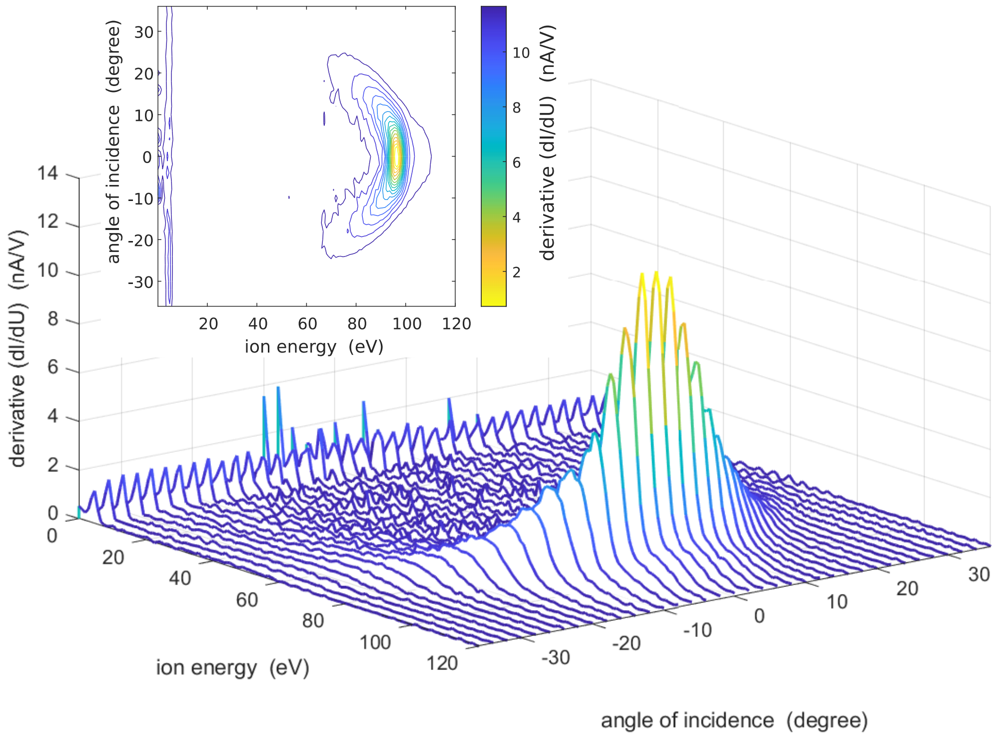

- solid lines U_{discr} = 40 V
- dashed lines U_{discr} = 0 V

RPA elastic scattering measurements

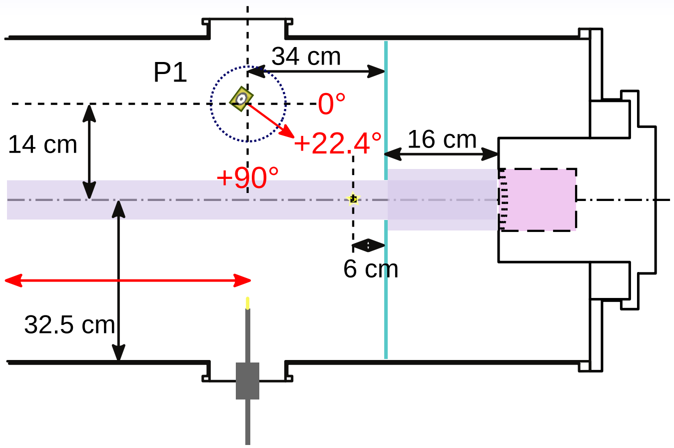

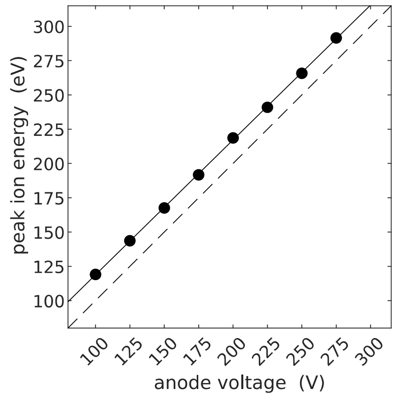

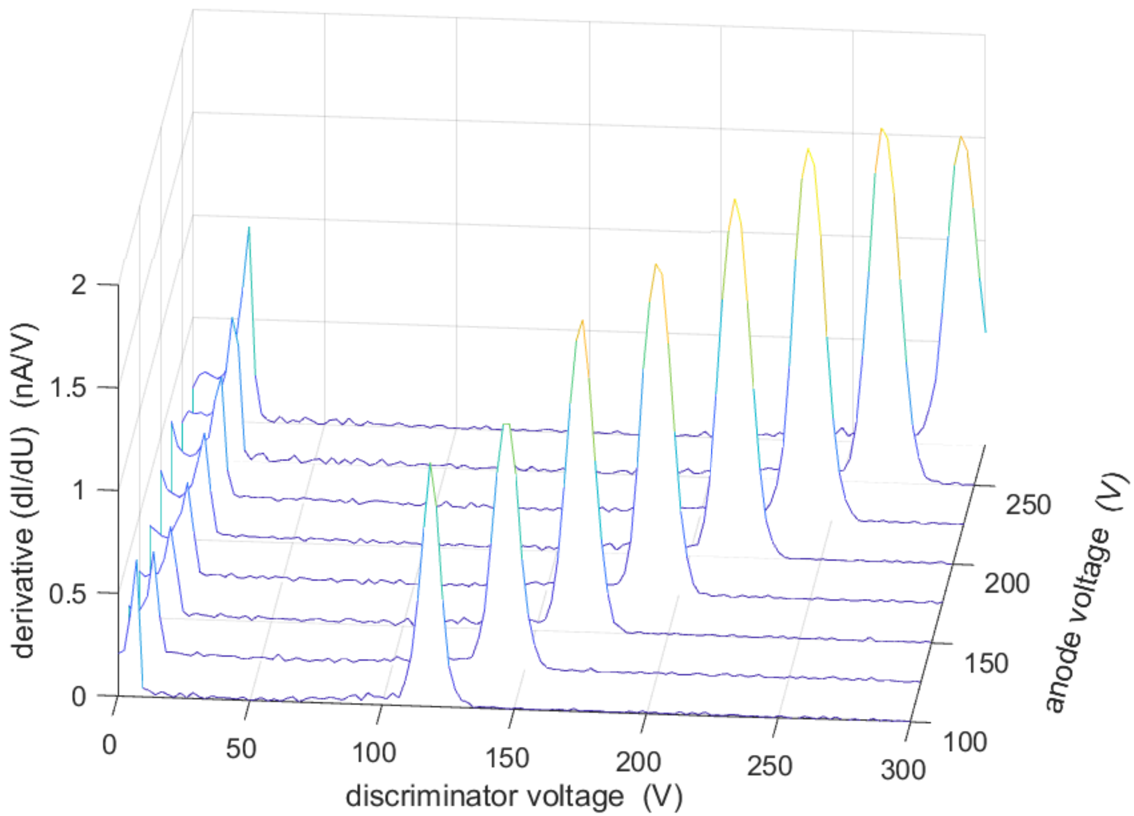

- purpose of this test is that the RPA may collect both charge-exchange ions and some of the elastically scattered ions
- such ions would retain most of their kinetic energy (part of the energy is transferred to the collision partner, a neutral Xe atom)
- ion energy is numerically about 17.4 eV higher than the corresponding anode voltage in V

Erosion Sensor Tests

Erosion Sensor

- meander is a 2 µm thick silver layer and a 200nm thick chromium layer sputtered onto a ceramic substrate
- ceramics were first cycled three times to -35°C and 65°C, then annealed for approx. 168h at 150°C
- during burn-in, the resistance of the Plasma-Test meander decreased from 36.58 Ω to 36.08 Ω

Erosion Sensor

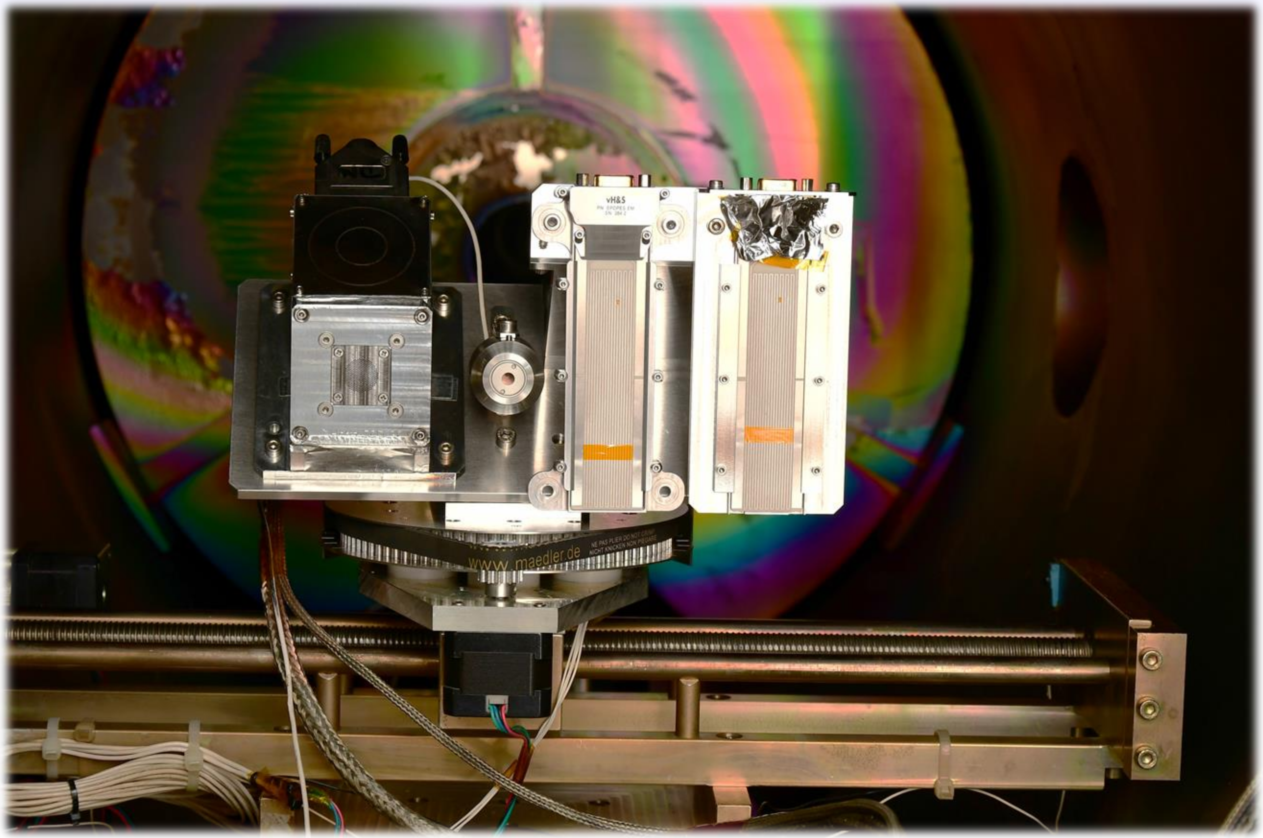

- sputtering by Xe with U_{anode} = 250 V @ 34 cm
- no hot cathode due to the heat transmission to the ES
- the FC is moved once in an hour into the beam center to measure the ion current density
- sensors were exposed 24 hours in three equal periods of 8 hours
- an erosion of roughly 1000 nm is expected

Erosion Sensor

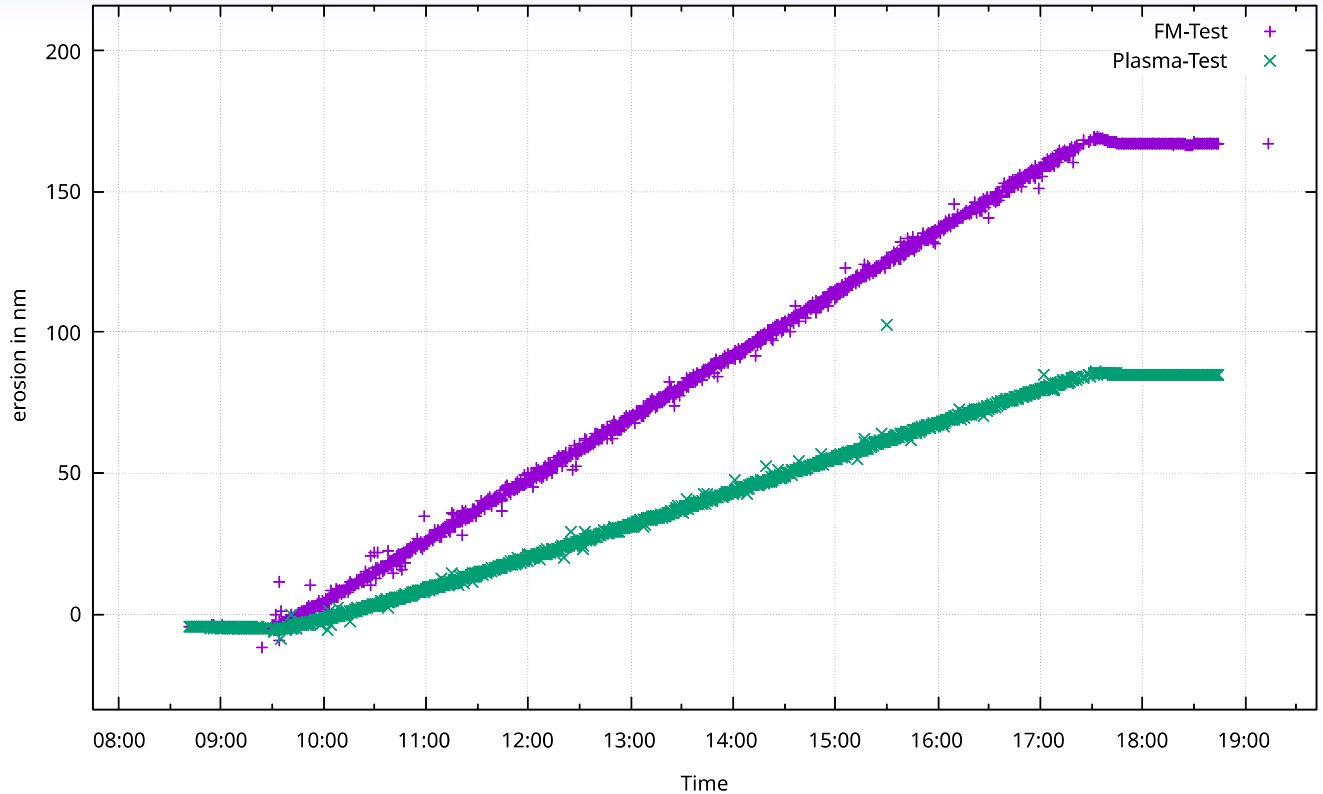

- live measurement during first day with plasma with EM E-Box

	Ag [nm] Initial	Ag [nm] After 2 Plasma	Δ [nm]
FM-Test	2250	1499	751
Plasma-Test	2640	2161	479

- mean measured silver layer thickness of the FM-Test and Plasma-Test ES with X-ray confocal microscope

Thank you for your attention